

A Technique to Transfer Metallic Nanoscale Patterns to Small and Non-Planar Surfaces

Elizabeth J. Smythe,[†] Michael D. Dickey,^{*} George M. Whitesides,^{*,*} and Federico Capasso[†]

[†]School of Engineering and Applied Sciences, Harvard University, 29 Oxford Street, Cambridge, Massachusetts 02138, and [‡]Department of Chemistry and Chemical Biology, Harvard University, 12 Oxford Street, Cambridge, Massachusetts 02138

Nanostructures exhibit optical,¹ thermal,² electrical,³ and magnetic⁴ properties that differ from bulk materials. To harness these properties into functional devices, it is often important to control their size, shape, and position on a substrate. Electron-beam (e-beam) lithography has one of the highest resolutions of the lithographic techniques; it is often used to define nanostructures, as it can pattern arbitrary features over large areas (>1 cm²) with a resolution of approximately 10 nm.⁵ E-beam patterning of non-planar surfaces (e.g., microspheres, lenses, cylinders, atomic-force microscope (AFM) tips) is challenging because these substrates are difficult to coat evenly with resist and because their surfaces do not lie in a single focal plane for the e-beam. E-beam patterning on extremely small planar substrates (e.g., fiber and laser facets, small pieces of substrates) is also challenging, as the edge bead resulting from the coating of resist can be as large as the sample itself. Evaporative e-beam resists that eliminate edge beads have been developed but require the use of an evaporation chamber with specific design and vacuum requirements, as well as specialized resist and developer.⁶

Focused-ion beam (FIB) milling is a high-resolution patterning technique that sculpts features by bombarding substrates with high-energy gallium ions. It has been used to pattern small, planar substrates^{7–12} because it does not require the use of resist. FIBs, however, are not widely available and, like e-beam writers, the gallium ion beam is focused on a single plane. FIB milling also implants gallium ions into the sculpted surface and thus has the potential to affect the optical and electronic properties of the resulting substrate.¹³

ABSTRACT Conventional lithographic methods (e.g., electron-beam lithography, photolithography) are capable of producing high-resolution structures over large areas but are generally limited to large (>1 cm²) planar substrates. Incorporation of these features on unconventional substrates (i.e., small (<1 mm²) and/or non-planar substrates) would open possibilities for many applications, including remote fiber-based sensing, nanoscale optical lithography, three-dimensional fabrication, and integration of compact optical elements on fiber and semiconductor lasers. Here we introduce a simple method in which a thin thiol-ene film strips arbitrary nanoscale metallic features from one substrate and is then transferred, along with the attached features, to a substrate that would be difficult or impossible to pattern with conventional lithographic techniques. An oxygen plasma removes the sacrificial film, leaving behind the metallic features. The transfer of dense and sparse patterns of isolated and connected gold features ranging from 30 nm to 1 μm, to both an optical fiber facet and a silica microsphere, demonstrates the versatility of the method. A distinguishing feature of this technique is the use of a thin, sacrificial film to strip and transfer metallic nanopatterns and its ability to directly transfer metallic structures produced by conventional lithography.

KEYWORDS: pattern transfer · soft lithography · metal nanoparticles · nanofabrication · nanopatterning

Soft lithographic techniques, which use an elastomeric (typically poly(dimethylsiloxane) (PDMS)) stamp to pattern features, can be used to define metallic features on planar and curved substrates.^{14–17} Micro-contact printing (μCP) is a soft lithographic method in which the substrate is “inked” by a stamp with a self-assembled monolayer that defines the printed pattern and has been used to pattern lenses, capillaries, and the sides of an optical fiber.^{14–17} The resolution of reproducible μCP is generally considered to be ~0.1–0.2 μm because of ink diffusion and stamp deformation,¹⁸ although some smaller trenches have been etched in planar metal surfaces.¹⁹ Patterns of thin metal features have been made by nanotransfer printing (nTP),^{20,21} a method in which metal is deposited onto an elastomeric stamp with topographical features and then printed onto a final substrate. Typically, the transfer of metal to the substrate is facilitated by an interfacial

*Address correspondence to gwhitesides@gmwhgroup.harvard.edu.

Received for review October 29, 2008 and accepted December 17, 2008.

Published online December 30, 2008. 10.1021/nn800720r CCC: \$40.75

© 2009 American Chemical Society

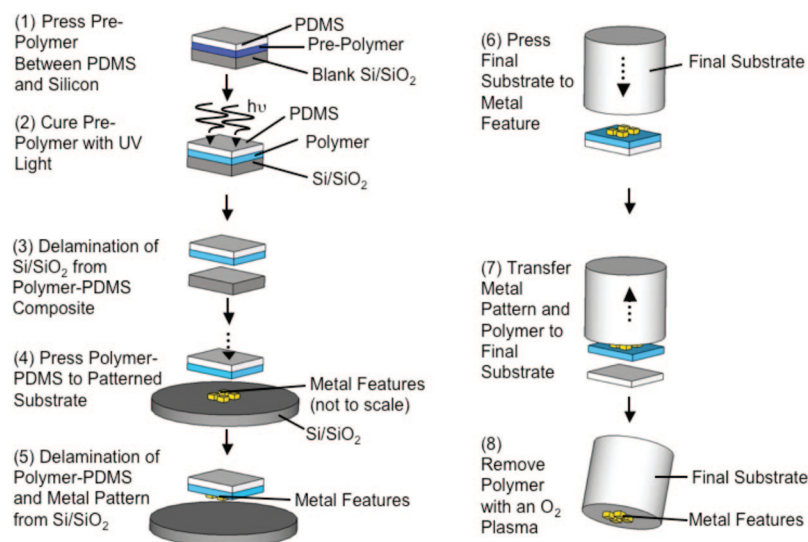


Figure 1. Schematic depiction of the procedure for transferring metallic nanostructures: (1) press the thiol-ene prepolymer between a featureless silicon wafer and extracted PDMS, (2) UV cure the thiol-ene prepolymer to make a thin thiol-ene polymer film, (3) delaminate the film–PDMS composite from the wafer in a DI water bath, (4) press the thiol-ene film–PDMS composite against a metallic nanopattern (not shown to scale), (5) delaminate the film–PDMS composite and the attached metal features from the silicon substrate in a DI water bath, (6) press the desired substrate (shown here as a cylinder) against the metallic pattern, (7) transfer the pattern and thiol-ene film to the final substrate, (8) remove the thiol-ene film with an O₂ plasma.

adhesion layer (e.g., a self-assembled monolayer or thin film of tacky polymer) between the two surfaces.

The elastomeric stamps used in relief-based, soft lithographic techniques (such as nTP and μ CP) allow the stamps to conform to the substrate, but the low Young's modulus of these stamps limits the geometry, registration, and aspect ratios of the printed features since the stamps can deform during patterning.^{18,22,23} Metal films deposited by physical vapor deposition onto elastomeric stamps can also crack and wrinkle due to differences in thermal expansion coefficients between the metal and stamp.²⁴ Increasing the modulus of the stamp (e.g., by using high-modulus PDMS) reduces feature deformation but decreases the flexibility and conformability of the stamp.^{25–29} Stamps incorporating high-modulus PDMS have been used to print 70 nm metal lines.²⁸

PDMS has also been used to transfer microscopic features kinetically from one substrate to another.³⁰ The ability to transfer features depends on the kinetic adhesion between the PDMS, the features, and the substrates; this method requires specific control of the contact time and adhesion forces between the PDMS and each individual feature. Kinetic adhesion has been used to transfer samples of varying size and composition (e.g., mica ribbons, graphite sheets, pollen grains,³⁰ silicon ribbons,^{31,32} gold electrodes,³³ and carbon nanotubes³⁴); however, there have been no reports of kinetic adhesion transfer being used to move patterns with nanoscale metallic features.

Arrays of self-assembled nanospheres have been used as stencil masks for the creation of nanoparticles

by physical vapor deposition (i.e., colloidal lithography³⁵) and have also been formed on small substrates (e.g., fiber facets³⁶), but this self-assembly-based method is limited to the formation of close-packed particle arrays and is susceptible to defects during assembly.³⁵

We sought a method to harness the high resolution and geometric versatility of e-beam lithography and the topographical adaptability of polymer-based “soft” nanofabrication methods to transfer arbitrary metallic nanopatterns to various unconventional substrates. The method we describe here is distinguished by offering (i) high feature and spacing resolution, limited only by the resolution of e-beam lithography, (ii) a wide range of transferable pattern geometries and aspect ratios, as it does not suffer from the elastomeric stamp limitations of many soft lithographic methods, and (iii) no residual doping from ion implantation, as occurs in focused-ion beam milling.

RESULTS AND DISCUSSION

Process Design. The transfer method uses a thin, sacrificial thiol-ene film to strip metallic features from a patterned substrate (Figure 1). Both the film and the features are subsequently transferred to a final substrate, and the sacrificial film is etched away, leaving behind the desired metallic nanopattern.

Nanofeatures: We defined the nanofeatures using e-beam lithography because it can define arbitrary patterns with high resolution (\sim 10 nm) and then performed e-beam evaporation (with no metallic adhesion layer) and standard lift-off. Scanning-electron microscope (SEM) inspection of a typical sample shows \sim 99% yield of features after lift-off. We patterned gold on a Si/SiO₂ substrate (silicon with a native oxide layer) because the van der Waals forces between the gold and the Si/SiO₂ substrate are strong enough to withstand lift-off following e-beam patterning but weak enough to allow the features to be stripped off by the thiol-ene film.

Thiol-ene Film Preparation: We used a sacrificial, polymer (thiol-ene) film bearing thiol groups to strip the metallic features (defined by e-beam lithography) from the substrate. We engineered this thiol-ene film to have the following properties: (i) to be thin (\sim 200 nm) and flexible, (ii) to be removable sacrificially by oxygen plasma, (iii) to be photocurable, and (iv) to have components that are commercially available and convenient to process.

The thiol-ene film consisted of 1:1:2 weight ratio of 2-bis(prop-2-enoyloxymethyl)butoxymethyl]-2-(prop-2-enoyloxymethyl)butyl]prop-2-enoate (“ene”)/[3-(3-sulfanylpropanoyloxy)-2,2-bis(3-sulfanylpropanoyloxymethyl)propyl]3-sulfanylpropanoate

("thiol")/1-methoxypropan-2-yl acetate (PGMEA, Sigma Aldrich) with ~1 wt % of radical photoinitiator (Irgacure 754, Ciba Specialty Chemicals). The thiol and ene are photocurable by a free radical polymerization and are both multifunctional, thereby cross-linking the cured film. We incorporated thiol groups into the film to promote adhesion to the metallic features. The PGMEA lowers the solution viscosity to facilitate spreading (explained below) of the thiol-ene monomer solution to ensure that the film will be thin; this sacrificial thiol-ene film has to be thin because it is ultimately removed from the final substrate by oxygen plasma.

We placed the thiol-ene monomer solution between a blank silicon wafer and a piece of PDMS and compressed the stack to create a thin layer of thiol-ene monomer solution between the silicon and PDMS (step 1). We cured the thiol-ene monomer solution by irradiating it with light through the PDMS (step 2). Typically, the resulting thiol-ene films ranged from 200 to 300 nm in thickness, as determined by profilometry. We cured the thiol-ene film between the PDMS and a blank silicon wafer, rather than curing it directly on the features, to prevent shrinkage of the curing thiol-ene monomer mixture from distorting the metallic pattern.

The PDMS served as a macroscopic intermediate substrate to facilitate the handling of the cured thin thiol-ene film. We used extracted PDMS to prevent uncross-linked PDMS oligomers from contaminating the thiol-ene film with unwanted silane residue.³⁷ We chose PDMS because of the ease with which it can be separated mechanically from the thin film of thiol-ene polymer (we could peel the cured thiol-ene from the PDMS). This ease of separation is beneficial during the final processing step in which we transfer the thiol-ene film (bearing the metal features) to the desired substrate. All of the other processing steps, however, require that the thiol-ene film and PDMS remain laminated. We developed the process to prevent this delamination prior to the final pattern transfer.

Thin-Film Manipulation: The cured thiol-ene film must be released from the silicon substrate and remain attached to the PDMS, so that it can be used to strip the metal features patterned by e-beam lithography. Unfortunately, the PDMS delaminates at the PDMS–film interface when it is mechanically peeled away from the silicon substrate. To promote separation at the PDMS–silicon interface (and prevent premature separation at the PDMS–film interface), we placed the stacked structure in a deionized (DI) water bath (step 3). Separation between the edges of the PDMS–film composite and the wafer occurred after soaking in the bath for ~45 min, after which gentle prodding completely removed the composite from the silicon substrate; soaking for ~24 h usually resulted in complete delamination of the film–PDMS composite from the silicon. We believe this selective delamination occurred

because the silicon wafer is hydrophilic, whereas the PDMS is hydrophobic.

Stripping the Features: After drying the PDMS–film composite gently with nitrogen, we pressed the thiol-ene film onto the silicon wafer patterned with gold nanostructures (formed by conventional e-beam lithography, gold evaporation, and liftoff) (step 4). We applied light pressure to the PDMS to promote strong bond formation between the gold nanostructures and extra thiol groups in the film (achieved by using an excess of thiol groups relative to ene groups in the thiol-ene formulation). When placed in a (second) DI water bath, the thiol-ene film again delaminated at the film–silicon interface, but stayed attached to the PDMS. The thiol-ene film stripped the patterns of gold features from the Si/SiO₂ substrate and transferred them to the film/PDMS composite (step 5).

Feature Transfer: To transfer the thiol-ene film (bearing the nanofeatures) from the intermediate PDMS substrate to the final substrate, we used a stereoscope to align the final substrate over the metallic pattern and gently pressed down to contact the final substrate surface and the metal features on the thiol-ene film (step 6). The elastomeric properties of PDMS helped to promote contact between the metal features and the final substrate. Both the metal features and the thiol-ene film released from the PDMS and transferred to the final substrate (step 7). We placed the substrate in a vacuum oven to promote better contact between the substrate surface and the metal features on the thiol-ene film. We then removed the sacrificial film with an oxygen plasma, leaving the pattern of gold nanostructures (originally created by e-beam lithography) attached to the final substrate (step 8). We found that the gold features transferred to the substrate regardless of whether the substrate was functionalized (*e.g.*, to bear thiol groups) prior to the pattern transfer. The Supporting Information contains details of an optional surface functionalization that can be used to promote adhesion between the final substrate and the metallic structures.

To demonstrate the versatility of the technique, we chose two final substrates that are difficult to pattern with conventional lithographic techniques: the facet of an optical fiber, which is small and planar (125 μm in diameter), and a small and non-planar silica microsphere, which is ~220 μm in diameter. We also transferred gold and silver features ranging from 30 nm to 1 μm in size and have shown that the technique can transfer both dense and sparse patterns, as well as isolated and connected features.

Transfer Results. Figure 2 is a series of scanning-electron microscope (SEM) images showing an array of gold nanorods transferred to the optical fiber facet. Figure 2a is a close-up of a section of the transferred array, while Figure 2b,c shows a SEM image and a sketch of the alignment of the array on the fiber facet, respectively. The transferred pattern is the same as the origi-

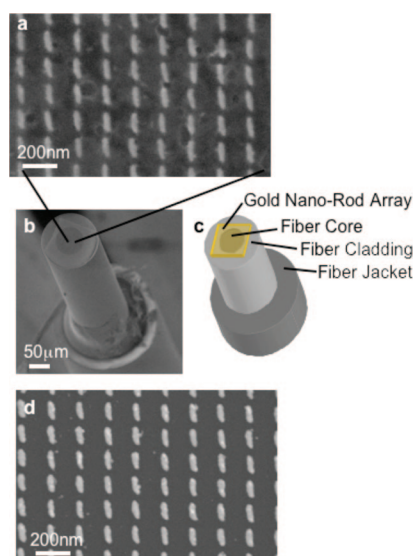


Figure 2. (a) SEM micrograph showing a section of a gold nanorod array transferred to the facet of an optical fiber. (b) SEM image of a transferred nanorod array on the facet of an optical fiber. (c) Schematic illustrating the arrays on the fiber facet. (d) Image of nanorods on a silicon substrate before the transfer. The images of the transferred arrays in (a) are of lower resolution than those of the arrays on silicon (d) due to charging of the silica microsphere.

nal created by e-beam lithography (Figure 2d), a $100\ \mu\text{m} \times 100\ \mu\text{m}$ array of gold nanorods, each approximately $40\ \text{nm}$ tall, $100\ \text{nm}$ long, and $30\ \text{nm}$ wide. The structures are separated by gaps of approximately $30\ \text{nm}$ along their long axis and $150\ \text{nm}$ along their short axis. The circle in the middle of the facet is the fiber core ($62.5\ \mu\text{m}$ in diameter), and the region surrounding it is the cladding ($125\ \mu\text{m}$ in diameter). Although we aligned the fiber and array by hand, the nanorods consistently covered the fiber core on different samples. The textured background in Figure 2a results from oxygen plasma etching and is found on sections of the fiber both with and without the transferred nanorods, as well as pristine cleaved fiber surfaces.

Figure 3 shows SEM images of a gold nanorod array transferred to the surface of a silica microsphere (diameter $\sim 220\ \mu\text{m}$). Figure 3a is a close-up of the nanorod array on the microsphere, while the SEM image and schematic in Figure 3b,c show the transferred array on the microsphere substrate. Figure 3d shows a section of the pattern on silicon before the transfer. The gold rods in Figure 3 are approximately $85\ \text{nm}$ in length, $45\ \text{nm}$ in width, $40\ \text{nm}$ tall, with gaps of $20\ \text{nm}$ along the rod length and $110\ \text{nm}$ along the rod width, and were written with e-beam lithography over a $100\ \mu\text{m} \times 100\ \mu\text{m}$ area. On the basis of SEM examination, there is minimal pattern distortion of the transferred array since the sphere radius is large enough for the surface to be approximately planar over localized areas.

To demonstrate the versatility of the technique, we transferred various metallic patterns of different sizes and pattern densities. Figure 4 shows SEM images of di-

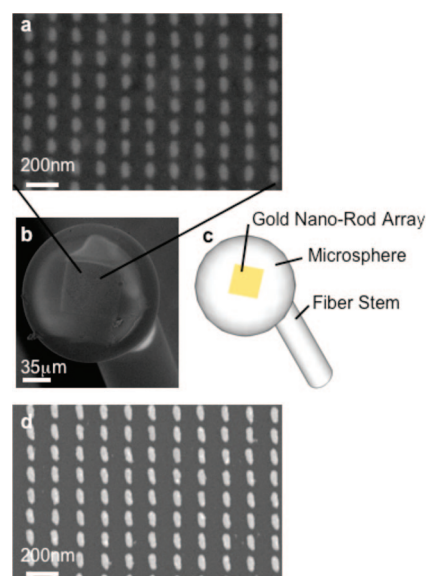


Figure 3. (a) SEM micrograph showing a section of a gold nanorod array transferred to the surface of a silica microsphere. (b) SEM image of an array of nanorods transferred to a microsphere. (c) Schematic illustrating the position of the transferred arrays. (d) Image of nanorods on a silicon substrate before being transferred. The images of the transferred arrays in (a) are of lower resolution than those of the arrays on silicon (d) due to charging of the silica microsphere.

verse patterns of gold on the facets of optical fibers. Figure 4a shows an array of $1\ \mu\text{m} \times 1\ \mu\text{m}$ gold squares, each $40\ \text{nm}$ tall, separated by $9\ \mu\text{m}$ in one direction and $1\ \mu\text{m}$ in the other. These squares have an aspect ratio length/height and width/height of ~ 25 , and a spacing ratio (spacing/height) of ~ 225 . The pattern in Figure 4b is a series of gold lines intersecting at 45° and 90° angles, each $\sim 100\ \text{nm}$ wide, $100\ \mu\text{m}$ long, $40\ \text{nm}$ tall, spaced at $10\ \mu\text{m}$. These intersecting lines were written as a continuous pattern, which remained unbroken when transferred to the fiber facet. Figure 4c shows gold split ring resonators, key building blocks of three-dimensional meta-materials,^{38,39} which are $\sim 420\ \text{nm}$ on each side, $40\ \text{nm}$ tall, have a gap of $60\ \text{nm}$, a wire width of $60\ \text{nm}$, and are separated by $\sim 480\ \text{nm}$.

The structures shown in Figures 2–4 are a sampling of patterns that can be transferred by this thiolene film-based technique. In principle, the shapes and spacing of the transferred structures are limited only by the techniques used to form them: electron-beam lithography should allow for large areas of transferred patterns with structures and spacings $10\ \text{nm}$ and smaller.

We have repeated the transfer procedure (Figure 1) multiple times on both fiber facets and microspheres and have an overall $\sim 80\%$ rate of achieving successful transfers; we define “successful” as any time a film and pattern are transferred cleanly to the final substrate. In most “unsuccessful” attempts, the thiol-ene film and pattern stay on the PDMS rather than transfer to the final substrate, or the film is wrinkled in the transfer pro-

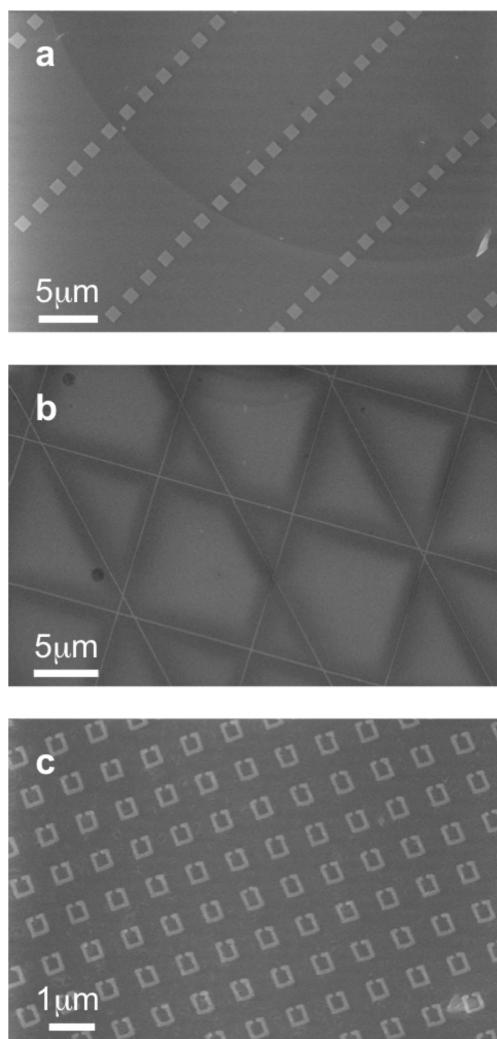


Figure 4. Various gold patterns transferred to a fiber facet: (a) SEM micrograph of $1\ \mu\text{m} \times 1\ \mu\text{m}$ squares, 40 nm tall, separated by 9 and $1\ \mu\text{m}$. The dark curve running through the image is the boundary between core and cladding of the fiber; (b) 100 nm wide and 40 nm tall lines, 100 μm long, spaced by $10\ \mu\text{m}$, at 45 and 90° angles. These features were written as one continuous pattern and remain connected after the transfer, with no tears or rips. (c) Split ring resonators with sides 420 nm long, 40 nm tall, and line widths of 80 nm. Each resonator has a 60 nm gap, and they are spaced by 480 nm.

cess. After a successful transfer, we observe a defect rate less than 1% (e.g., in a transferred $100\ \mu\text{m} \times 100\ \mu\text{m}$ array of nanorods, less than 1% of the rods are missing or misaligned). These defects usually occur in areas where the final substrate is rough or dirty. We attribute part of this low defect rate to the thiol-ene film, which acts as a “backbone” supporting the metallic nanofea-

tures; the thiol-ene film moves to the final substrate as a continuous sheet. The thiol-ene film (bearing the nanostructures)—which separates readily from the PDMS backing—transfers to the desired substrate without prefunctionalizing the substrate. The metallic features, therefore, are in direct contact with the desired substrate and are presumably held in place by van der Waals forces. This capability may be beneficial for applications in which an intermediate adhesion layer is detrimental or not an option.

We successfully transferred patterns of both gold and silver. This transfer method should be immediately applicable to other metals, such as platinum and palladium, which bind to thiols strongly and to silicon weakly. This technique could be adapted to other materials by proper selection of substrates and design of interfacial chemistry. Eligible materials must (i) be able to be patterned on a flat substrate without forming covalent bonds with the substrate and (ii) have a surface functionality that allows the material to be stripped. For example, replacement of the thiol groups with long-chain hydroxamic acids or phosphonic acids could allow for the transfer of metals that form native oxides and do not bind strongly to thiols.^{40,41}

CONCLUSION

We presented a nanofabrication method that allows metallic structures created with electron-beam lithography to be transferred to unconventional substrates (i.e., small ($<1\ \text{mm}^2$) and/or non-planar) that are difficult to pattern with standard lithographic techniques. We demonstrated the transfer of a variety of gold patterns and features to both the facet of an optical fiber and to the curved surface of a silica microsphere without functionalizing the surfaces of these substrates. This straightforward method could be adapted to transfer patterns made out of different materials to various types of unconventional substrate geometries and compositions.

This transfer technique may be useful for the development of new devices, such as fiber-based probes for sensing and detection,^{12,36,42} optical elements integrated onto lasers and optical devices,^{9–11} and frequency selective surfaces.^{38,39,43} The technique also could lead to advances in nanoscale optical lithography,⁴⁴ stacking of features for three-dimensional fabrication, and the patterning of non-planar elements designed to fit into areas with space constraints.

METHODS

Fabrication of Metallic Features. We fabricated the metallic features using e-beam lithography and lift-off. We spin-coated a silicon wafer with two layers of PMMA (MicroChem Corp), 495 A2 and 950 A2, respectively, and baked the substrate at 150 °C for 10 min after each coating. We patterned the resist by e-beam li-

thography (JEOL 7000, 30 keV) and developed it using MIBK/IPA 1:3 developer (MicroChem). We e-beam-evaporated gold or silver onto the samples (without a metal adhesion layer) and submerged the samples in acetone to remove the excess metal and resist.

Creation of Polymer Film. We placed 5 μL of the thiol-ene monomer solution between a blank silicon wafer and a $1\ \text{cm} \times 1\ \text{cm}$

piece of extracted PDMS and clamped the film. The thiol-ene monomer solution was UV cured through the PDMS for 10 min using a mercury lamp (100 W bulb, at a distance of ~15 cm).

Delamination in DI Water Bath. Prior to submerging the stack in the water bath, we cleaved the silicon wafer around the edges of the PDMS (exposing fresh silicon film interfaces) to help accelerate the delamination.

The film–PDMS composite was pressed against the nanopatterned silicon wafer for 10 min to promote strong bonding between the gold particles and the thiol groups in the film.

Post Feature-Transfer Processing. After transferring the metal features and film to the unconventional substrates, the samples were baked in a vacuum oven at 125 °C for 1 h. The sacrificial thin polymer film was removed by an oxygen plasma (60 W, 350 mT, 5 min).

Acknowledgment. E.J.S. and F.C. are supported by the MEMS/NEMS:Science & Technology Fundamentals Program supported by Defense Advanced Research Projects Agency under Award No. HR0011-06-1-0044. G.M.W. is supported by the California Institute of Technology Center for Optofluidic Integration supported by the Defense Advanced Research Projects Agency under award number HR0011-04-1-0032, and the National Institutes of Health under contract NIEHS # ES016665. This work was performed in part at the Center for Nanoscale Systems (CNS) at Harvard University, a member of the National Nanotechnology Infrastructure Network (NNIN). The authors thank R. Chiechi, S. Thomas, and N. Clay for their valuable discussions.

Supporting Information Available: Details of an optional surface functionalization that can be used to promote adhesion between the final substrate and the metallic structures. This material is available free of charge via the Internet at <http://pubs.acs.org>.

REFERENCES AND NOTES

- Bohren, C. F.; Huffman, D. R. *Absorption and Scattering of Light by Small Particles*; John Wiley & Sons: New York, 1983.
- Buffat, P.; Borel, J. P. Size Effect on Melting Temperature of Gold Particles. *Phys. Rev. A* **1976**, *13*, 2287–2298.
- Andres, R. P.; Bielefeld, J. D.; Henderson, J. I.; Janes, D. B.; Kolagunta, V. R.; Kubiak, C. P.; Mahoney, W. J.; Osifchin, R. G. Self-Assembly of a Two-Dimensional Superlattice of Molecularely Linked Metal Clusters. *Science* **1996**, *273*, 1690–1693.
- Shi, J.; Gider, S.; Babcock, K.; Awschalom, D. D. Magnetic Clusters in Molecular Beams, Metals, and Semiconductors. *Science* **1996**, *271*, 937–941.
- Wang, H.; Laws, G. M.; Milicic, S.; Boland, P.; Handugan, A.; Pratt, M.; Eschrich, T.; Myhajlenko, S.; Allgair, J. A.; Bunday, B. Low Temperature ZEP-520A Development Process for Enhanced Critical Dimension Realization in Reactive Ion Etch Etched Polysilicon. *J. Vac. Sci. Technol., B* **2007**, *25*, 102–105.
- Kelkar, P. S.; Beauvais, J.; Lavallee, E.; Drouin, D.; Cloutier, M.; Turcotte, D.; Yang, P.; Mun, L. K.; Legario, R.; Awad, Y.; et al. Nano Patterning on Optical Fiber and Laser Diode Facet with Dry Resist. *J. Vac. Sci. Technol., A* **2004**, *22*, 743–746.
- Chen, F.; Itagi, A.; Bain, J. A.; Stancil, D. D.; Schlesinger, T. E.; Stebounova, L.; Walker, G. C.; Akhremitchev, B. B. Imaging of Optical Field Confinement in Ridge Waveguides Fabricated on Very-Small-Aperture Laser. *Appl. Phys. Lett.* **2003**, *83*, 3245–3247.
- Partovi, A.; Peale, D.; Wuttig, M.; Murray, C. A.; Zydzik, G.; Hopkins, L.; Baldwin, K.; Hobson, W. S.; Wynn, J.; Lopata, J.; et al. High-Power Laser Light Source for Near-Field Optics and Its Application to High-Density Optical Data Storage. *Appl. Phys. Lett.* **1999**, *75*, 1515–1517.
- Yu, N.; Cubukcu, E.; Diehl, L.; Belkin, M. A.; Crozier, K. B.; Capasso, F.; Bour, D.; Corzine, S.; Hoffer, G. Plasmonic Quantum Cascade Laser Antenna. *Appl. Phys. Lett.* **2007**, *91*, 173113-1–173113-3.
- Yu, N. F.; Cubukcu, E.; Diehl, L.; Bour, D.; Corzine, S.; Zhu, J. T.; Hoffer, G.; Crozier, K. B.; Capasso, F. Bowtie Plasmonic Quantum Cascade Laser Antenna. *Opt. Express* **2007**, *15*, 13272–13281.
- Cubukcu, E.; Kort, E. A.; Crozier, K. B.; Capasso, F. Plasmonic Laser Antenna. *Appl. Phys. Lett.* **2006**, *89*, 093120-1–093120-3.
- Smythe, E. J.; Cubukcu, E.; Capasso, F. Optical Properties of Surface Plasmon Resonances of Coupled Metallic Nanorods. *Opt. Express* **2007**, *15*, 7439–7447.
- Fu, Y. Q.; Bryan, N. K. A. Investigation of Physical Properties of Quartz After Focused Ion Beam Bombardment. *Appl. Phys. B* **2005**, *80*, 581–585.
- Rogers, J. A.; Jackman, R. J.; Whitesides, G. M. Microcontact Printing and Electroplating on Curved Substrates: Production of Free-Standing Three-Dimensional Metallic Microstructures. *Adv. Mater.* **1997**, *9*, 475–477.
- Rogers, J. A.; Jackman, R. J.; Whitesides, G. M. Constructing Single- and Multiple-Helical Microcoils and Characterizing Their Performance as Components of Microinductors and Microelectromagnets. *IEEE JMEMS* **1997**, *6*, 184–192.
- Rogers, J. A.; Jackman, R. J.; Whitesides, G. M.; Wagener, J. L.; Vengsarkar, A. M. Using Microcontact Printing to Generate Amplitude Photomasks on the Surfaces of Optical Fibers: A Method for Producing In-Fiber Gratings. *Appl. Phys. Lett.* **1997**, *70*, 7–9.
- Jackman, R. J.; Wilbur, J. L.; Whitesides, G. M. Fabrication of Submicrometer Features on Curved Substrates by Microcontact Printing. *Science* **1995**, *269*, 664–666.
- Xia, Y. N.; Whitesides, G. M. Soft Lithography. *Angew. Chem., Int. Ed.* **1998**, *37*, 551–575.
- Biebuyck, H. A.; Larsen, N. B.; Delamarche, E.; Michel, B. Lithography Beyond Light: Microcontact Printing with Monolayer Resists. *IBM J. Res. Dev.* **1997**, *41*, 159–170.
- Loo, Y. L.; Willett, R. L.; Baldwin, K. W.; Rogers, J. A. Additive, Nanoscale Patterning of Metal Films with a Stamp and a Surface Chemistry Mediated Transfer Process: Applications in Plastic Electronics. *Appl. Phys. Lett.* **2002**, *81*, 562–564.
- Loo, Y. L.; Willett, R. L.; Baldwin, K. W.; Rogers, J. A. Interfacial Chemistries for Nanoscale Transfer Printing. *J. Am. Chem. Soc.* **2002**, *124*, 7654–7655.
- Delamarche, E.; Schmid, H.; Michel, B.; Biebuyck, H. Stability of Molded Polydimethylsiloxane Microstructures. *Adv. Mater.* **1997**, *9*, 741–746.
- Hsia, K. J.; Huang, Y.; Menard, E.; Park, J. U.; Zhou, W.; Rogers, J.; Fulton, J. M. Collapse of Stamps for Soft Lithography Due to Interfacial Adhesion. *Appl. Phys. Lett.* **2005**, *86*, 154106-1–154106-3.
- Bowden, N.; Brittain, S.; Evans, A. G.; Hutchinson, J. W.; Whitesides, G. M. Spontaneous Formation of Ordered Structures in Thin Films of Metals Supported on an Elastomeric Polymer. *Nature* **1998**, *393*, 146–149.
- Guo, L. J. Nanoimprint Lithography: Methods and Material Requirements. *Adv. Mater.* **2007**, *19*, 495–513.
- Chou, S. Y.; Krauss, P. R. Imprint Lithography with Sub-10 nm Feature Size and High Throughput. *Microelectron. Eng.* **1997**, *35*, 237–240.
- Pina-Hernandez, C.; Kim, J. S.; Guo, L. J.; Fu, P. F. High-Throughput and Etch-Selective Nanoimprinting and Stamping Based on Fast-Thermal-Curing Poly(dimethylsiloxane)s. *Adv. Mater.* **2007**, *19*, 1222–1227.
- Kang, M. G.; Kim, M. S.; Kim, J.; Guo, L. J. Organic Solar Cells Using Nanoimprinted Transparent Metal Electrodes. *Adv. Mater.* **2008**, *20*, 1–6.
- Kang, M. G.; Guo, L. J. Semitransparent Cu Electrode on a Flexible Substrate and Its Application in Organic Light Emitting Diodes. *J. Vac. Sci. Technol., B* **2007**, *25*, 2637–2641.
- Meitl, M. A.; Zhu, Z. T.; Kumar, V.; Lee, K. J.; Feng, X.; Huang, Y. Y.; Adesida, I.; Nuzzo, R. G.; Rogers, J. A. Transfer Printing by Kinetic Control of Adhesion to an Elastomeric Stamp. *Nat. Mater.* **2006**, *5*, 33–38.

31. Mack, S.; Meitl, M. A.; Baca, A. J.; Zhu, Z. T.; Rogers, J. A. Mechanically Flexible Thin-Film Transistors That Use Ultrathin Ribbons of Silicon Derived from Bulk Wafers. *Appl. Phys. Lett.* **2006**, *88*, 213101-1–213101-3.
32. Ko, H. C.; Baca, A. J.; Rogers, J. A. Bulk Quantities of Single-Crystal Silicon Micro-/Nanoribbons Generated from Bulk Wafers. *Nano Lett.* **2006**, *6*, 2318–2324.
33. Kim, J.; Khang, D. Y.; Kim, J. H.; Lee, H. H. The Surface Engineering of Top Electrode in Inverted Polymer Bulk-Heterojunction Solar Cells. *Appl. Phys. Lett.* **2008**, *92*, 093505-1–093505-3.
34. Aref, T.; Remeika, M.; Bezryadina, A. High-Resolution Nanofabrication Using a Highly Focused Electron Beam. *J. Appl. Phys.* **2008**, *104*, 024312-1–024312-6.
35. Hulteen, J. C.; Vanduyne, R. P. Nanosphere Lithography: a Materials General Fabrication Process for Periodic Particle Array Surfaces. *J. Vac. Sci. Technol., A* **1995**, *13*, 1553–1558.
36. Stokes, D. L.; Vo-Dinh, T. Development of an Integrated Single-Fiber SERS Sensor. *Sens. Actuators, B* **2000**, *69*, 28–36.
37. Lee, J. N.; Park, C.; Whitesides, G. M. Solvent Compatibility of Poly(dimethylsiloxane)-Based Microfluidic Devices. *Anal. Chem.* **2003**, *75*, 6544–6554.
38. Pendry, J. B.; Holden, A. J.; Robbins, D. J.; Stewart, W. J. Magnetism from Conductors and Enhanced Nonlinear Phenomena. *IEEE Trans. Microwave Theory Tech.* **1999**, *47*, 2075–2084.
39. Schurig, D.; Mock, J. J.; Justice, B. J.; Cumber, S. A.; Pendry, J. B.; Starr, A. F.; Smith, D. R. Metamaterial Electromagnetic Cloak at Microwave Frequencies. *Science* **2006**, *314*, 977–980.
40. Folkers, J. P.; Gorman, C. B.; Laibinis, P. E.; Buchholz, S.; Whitesides, G. M.; Nuzzo, R. G. Self-Assembled Monolayers of Long-Chain Hydroxamic Acids on the Native Oxides of Metals. *Langmuir* **1995**, *11*, 813–824.
41. Gao, W.; Dickinson, L.; Grozinger, C.; Morin, F. G.; Reven, L. Self-Assembled Monolayers of Alkylphosphonic Acids on Metal Oxides. *Langmuir* **1996**, *12*, 6429–6435.
42. Scheerlinck, S.; Taillaert, D.; Van Thourhout, D.; Baets, R. Flexible Metal Grating Based Optical Fiber Probe for Photonic Integrated Circuits. *Appl. Phys. Lett.* **2008**, *92*, 031104-1–031104-3.
43. Xu, Q. B.; Bao, J. M.; Rioux, R. M.; Perez-Castillejos, R.; Capasso, F.; Whitesides, G. M. Fabrication of Large-Area Patterned Nanostructures for Optical Applications by Nanoskiving. *Nano Lett.* **2007**, *7*, 2800–2805.
44. Sundaramurthy, A.; Schuck, P. J.; Conley, N. R.; Fromm, D. P.; Kino, G. S.; Moerner, W. E. Toward Nanometer-Scale Optical Photolithography: Utilizing the Near-Field of Bowtie Optical Nanoantennas. *Nano Lett.* **2006**, *6*, 355–360.